

Figure 2 Field-emission patterns from multi-walled carbon nanotubes. **a**, Field-emission pattern from closed-capped MWNTs. **b**, Field-emission pattern from open-ended MWNTs. The distance between the nanotube emitter (cathode) and the microchannel plate (anode) was 60 mm. The electric potential of the emitter against the grounded anode was -500 V for the closed tubes and -320 V for the open tubes.

purified MWNTs in the form of a black, thin 'mat' (a flake with a thickness of a few hundredths of a millimetre).

To make an electron emitter from capped MWNTs, we picked up a needle-like fragment (~ 0.1 mm diameter, 1–2 mm long) from the cathode deposit, and fixed it to a hairpin-shaped tungsten or nichrome wire (diameter 0.3 mm) using carbon paste. For the purified MWNTs, we cut out a thin thread (less than 0.1 mm wide, 1–2 mm long) with a sharp tip from the mat of MWNTs, using a razor, and attached a wire as before. We positioned the MWNT 60 mm in front of a microchannel plate, which had an effective diameter of 42 mm, and placed a fluorescent screen just behind the plate. The working pressure of the vacuum chamber for FEM was typically 2×10^{-9} torr, and the emitter tip was cooled to near liquid-nitrogen temperature. Emission patterns were recorded with a charge-coupled device (CCD) camera (Hamamatsu C5985).

We saw no inner structure in the capped MWNTs (Fig. 2a), but the open tubes showed a peculiar pattern of circular bright rings (Fig. 2b). In Fig. 2b there are two rings in contact with each other, corresponding to adjacent open tubes. A black spot in the central region — the absence of electrons in the core of a beam — corresponds to an exposed cavity. Diameters of inner black spots measured on the screen (2–3.5 mm) and the inner diameters of MWNTs (typically 5–10 nm) indicate an approximate magnification of one million for our FEM. As the electrons emitted from the tip are radially accelerated toward the screen, the beam from an open tube forms a hollow cone. The apex angles of the outer and inner cones of the hollow beam are about 0.2 and 0.05 radians, respectively. Using open-ended nanotubes we can produce a unique tubular configuration of the electron beam.

Rinzler *et al.*¹ claimed to have observed field emission from a linear carbon chain

pulled out from the open edge of a nanotube. Contrary to their report, we saw no sharp contrast corresponding to the atomic chain in our emission patterns. Electron emission seems to occur from the circular edges of the graphite layers of a nanotube.

Yahachi Saito, Koji Hamaguchi, Koichi Hata

Department of Electrical and Electronic Engineering, Mie University, Tsu 514, Japan
e-mail: saito@is.elec.mie-u.ac.jp

Kunio Uchida, Yoshiharu Tasaka

Fumikazu Ikazaki, Motoo Yumura
National Institute of Materials and Chemical Research, Tsukuba 305, Japan

Atsuo Kasuya, Yuichiro Nishina

Institute for Materials Research, Tohoku University, Sendai 980-77, Japan

1. Rinzler, A. G. *et al. Science* **269**, 1550–1553 (1995).
2. de Heer, W. A., Chatelain, A. & Ugarte, D. *Science* **270**, 1179–1180 (1995).
3. Collins, P. G. & Zettl, A. *Appl. Phys. Lett.* **69**, 1969–1971 (1996).
4. Gomer, R. *Field Emission and Field Ionization* Ch. 2 (Harvard Univ. Press, Cambridge, MA, 1961).
5. Ikazaki, F. *et al. in Proc. 211th ACS Natl Meeting Vol. 42* (eds Cronauer, D. C. *et al.*) 113–117 (Am. Chem. Soc., Washington DC, 1996).

DNA fingerprinting from single cells

Van Oorschot and Jones reported in *Scientific Correspondence*¹ that short tandem repeat (STR) profiles (DNA fingerprints) can be obtained from cells left on pens, car keys, and so on. Although this technique is a dramatic breakthrough with important implications for forensic science, there are two main limitations. First, more than 1 ng DNA (equivalent to 200 cells) is required; and second, a single STR locus is used, which does not provide much information. Here we report a system for

determining STR profiles from single cells using six forensic STR markers, which we believe is the first time that single cells have been typed using modern forensic techniques.

Genetic profiles can be obtained from single cells using an STR profiling system already in routine use in the United Kingdom, which gives a matching probability of roughly 1 in 50 million. The STR profile is reliable and accurate and is obtained within 5–6 hours.

We analysed 226 buccal cells from four different individuals, isolating each cell using micromanipulation procedures. DNA was amplified using a routine forensic identification system with modifications (different primer concentrations, Ampli-Taq Gold, and 34 cycles)². This system uses fluorescent polymerase chain reaction (PCR) amplification of six STR markers to provide an STR profile, and amelogenin to diagnose sex. We compared single-cell results to known STR profiles from the cell samples. We amplified DNA in 91% (206/226) cells, obtaining a full DNA profile in 50% (114/226) and an acceptable profile (four or more STRs) in 64% of these cells (Table 1). The remaining 27% of cells gave incomplete, partial profiles. Although these partial profiles may be insufficient for typing, they may provide sufficient information to exclude potential suspects.

These results show great promise and could be applied, for example, to smudged fingerprints, single flakes of dandruff, single sperm in multiple rape cases, and small samples left on weapons or vehicles (see ref. 1). However, they must be considered with some caution. Although we obtained an acceptable profile in almost two-thirds of cells tested, care must be taken with the interpretation of the results. Stochastic effects cause preferential amplification and

Table 1 Details of analysis

Number of single cells analysed	226
Results obtained	206 (91%)
Amplification failure	20 (9%)
Full STR profile	114 (50%)
Acceptable profile (amelogenin, ≥ 4 STRs)	144 (64%)
Partial profile (1–4 STRs)	62 (27%)
Surplus alleles*	28 (12%)
False alleles**	11 (5%)
Allele dropout	88 (39%)

*Additional allele present in conjunction with true alleles.

**Additional allele in place of true allele. Extra-allelic peaks could be caused by contamination, somatic mutation or PCR-generated non-allelic peaks. We never saw more than two additional peaks in a profile or in 18 negatives, minimizing the possibility of cellular contamination. When surplus alleles were observed we considered the locus, but not the profile, uninformative. We observed allele dropout in 39% of cells at a rate of $\sim 10\%$ in each allele. If two cells are analysed then the risk of allelic dropout and misinterpretation in cells is reduced to 1%, if three cells 0.1%, and so on. Wild-card designations and conservative statistical criteria are needed to ensure that evidential value can be properly assessed.

allele dropout³. Consequently, this technique requires validation before use in forensic casework. We are currently investigating a robust interpretation strategy for single-cell STR profiling. This work also raises issues about STR profiling low numbers of cells and the need for stringent precautions in collecting and processing to avoid contamination.

I. Findlay, A. Taylor, P. Quirke

Department of Molecular Oncology,
Algeron Firth Building, University of Leeds,
Leeds LS2 9LN, UK

R. Frazier, A. Urquhart

Forensic Science Service, Gooch Street North,
Birmingham B5 6QQ, UK

1. van Oorschot, R. A. H. & Jones, M. K. *Nature* **387**, 767 (1997).
2. Sparkes, R. *et al. Int. J. Legal Med.* **109**, 195–204 (1996).
3. Findlay, I., Ray, P., Quirke, P., Rutherford, A. J. & Lilford, R. *Hum. Reprod.* **10**, 1609–1618 (1996).

Archaeopteryx-like skull in Enantiornithine bird

The bird *Cathayornis* from the Early Cretaceous period gives the first evidence for a post-Jurassic survival of an *Archaeopteryx*-like skull in birds. This skull combines short, toothed premaxillaries, nasals meeting at the midline and submaxillary fossae in the antorbital fenestra.

During the late Mesozoic era, from the Early Cretaceous to the latest Cretaceous (Maestrichtian), two distinct groups of birds co-existed as separate lineages^{1,2}. One of these, the ornithurine birds, survived into the Cenozoic era to give rise to all modern birds^{3,4}. The other lineage, the Enantiornithes, became extinct along with dinosaurs at the end of the Cretaceous^{3,5}.

The structure of Enantiornithine bird skulls is poorly understood. Until now, the best known was *Gobipteryx*, of which there are fragmentary adult and embryonic skulls⁶ showing the absence of teeth, a reduced antorbital fenestra and an *Archaeopteryx*-like quadrate.

Cathayornis from the Early Cretaceous of China has the typical elongated outer metacarpal and the characteristic shapes of the scapula, coracoid, and distal tibiotarsus found in later enantiornithine birds^{3,7}. Photographs of the skull have been published⁸ and a drawing of it as it is preserved⁷, but there has been no detailed reconstruction of any enantiornithine skull published to date. Our reconstruction (Fig. 1) is based on the holotype of *Cathayornis* (specimen IVPP, V9769) and skulls from two skeletons referred to that genus (IVPP, V10896 and V10916). The latter two skulls provide information on the maxilla, lacrimal and a lateral view of the quadrate. The premaxilla bears four or five small teeth that are directed downwards or slightly forwards. It is covered externally with large nutrient foramina. The dorsal process of the premaxilla extends posteriorly slightly beyond the edge of the nares (nostrils). It is slightly shorter in *Archaeopteryx* (Fig. 1 c,d). The nares meet on the midline as in *Archaeopteryx* and are overlapped by the premaxillaries on their anterior process.

The premaxillaries are toothed and about one-third the length of the skull compared to about one-quarter in *Archaeopteryx*, and the nasals are shortened. The antorbital fenestra is large and triangular with two distinct anterior maxillary fossae. The maxillary is toothed. Teeth are set in sockets indicating that the individuals are mature. The teeth are not serrated and have

the expanded base and waisted crown typical of all known toothed birds (Fig. 1g). The 'T'-shaped lacrimal is inclined posteriorly. The braincase is expanded over that in *Archaeopteryx* (Fig. 1 b,d) and this may reflect an increased brain size coupled with an improved shoulder girdle (keeled sternum) and presumably more sophisticated powers of flight in *Cathayornis*. There is a bone in the posterior corner of the skull that might be a squamosal, but the quadrate articulation and basicranial region is not preserved in our material, nor is the quadratojugal and jugal.

There is a well-preserved quadrate (Fig. 1f) lying disarticulated and behind one skull (IVPP, V10916). It is a long slender bone with a single small proximal head and very little orbital process. It is similar to the quadrate (Fig. 1e) of the London, Eichstätt and seventh *Archaeopteryx* specimens⁹ and to that of *Gobipteryx*. In *Archaeopteryx* the dorsal process of the jugal is too far back to contact a postorbital even if one were present¹⁰. The reduction or loss of the postorbital frees the jugal bar for prokinesis and may have occurred more than once in avian evolution. *Cathayornis* lacks evidence for a postorbital but one is present in *Confuciusornis*. The flattened nature of the nasal and the nasal process of the premaxilla⁷ may also indicate the presence of prokinesis in *Cathayornis*.

If *Archaeopteryx* and the Enantiornithes are united into a monophyletic Sauriurae¹, then the presence of a primitive *Archaeopteryx*-like skull in *Cathayornis*, after the derived postcranial differences between enantiornithine and ornithurine birds was established, indicates that the modern ornithurine skull and 'typical avian kinesis' was developed independently by ornithurine birds.

**Larry D. Martin
Zhonghe Zhou***

Natural History Museum
and Department of Systematics and Ecology,
University of Kansas, Lawrence,
Kansas 66045, USA

*and Institute of Vertebrate Paleontology and
Paleoanthropology,
Chinese Academy of Sciences, PO Box 643,
Beijing 100044, China
e-mail: ldmartin@falcon.cc.ukans.edu

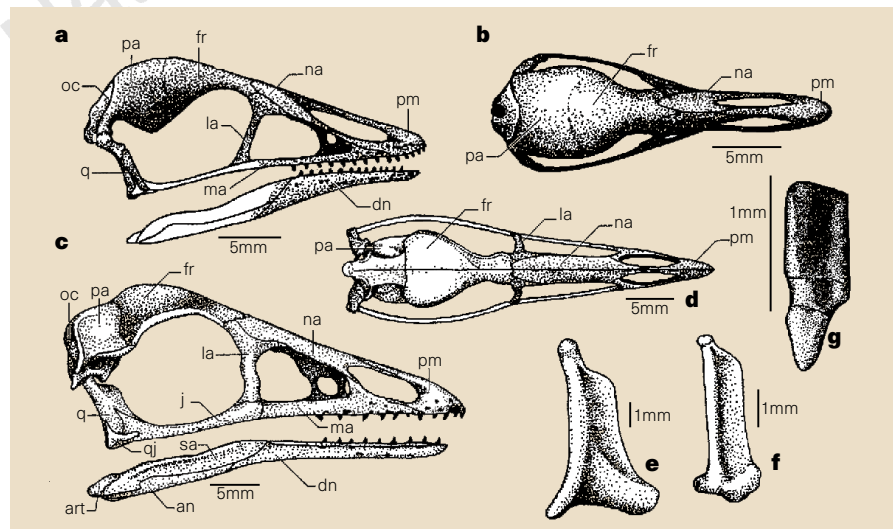


Figure 1 Reconstruction of skull structures of *Cathayornis* and *Archaeopteryx*. **a**, Lateral view of *Cathayornis*. **b**, Dorsal view of *Cathayornis*. **c**, Lateral view of *Archaeopteryx*. **d**, Dorsal view of *Archaeopteryx*. **e**, Quadrate of *Archaeopteryx*. **f**, Quadrate of *Cathayornis*. **g**, Labial view of tooth from the maxillary of *Cathayornis*. Abbreviations: an, angular; art, articular; dn, dentary; fr, frontal; j, jugal; la, lacrimal; ma, maxillary; na, nasal; oc, occipital; pa, parietal; pm, premaxillary; q, quadrate; qj, quadratojugal; sa, surangular.

1. Hou, L., Martin, L. D., Zhou, Z. & Feduccia, A. *Science* **274**, 1164–1167 (1996).
2. Martin, L. D. in *Origin of the Higher Groups of Tetrapods* (eds Schultze, H. P. & Trueb, L.) 485–540 (Comstock, Ithaca, 1991).
3. Martin, L. D. *Cour. Forschungsinst. Senckenberg* **181**, 23–36 (1995).
4. Feduccia, A. *The Origin and Evolution of Birds* (Yale Univ. Press, New Haven, 1996).
5. Chiappe, L. M. *Nature* **378**, 349–355 (1995).
6. Elzanowski, A. *Paleontol. Polon.* **42**, 147–179 (1981).
7. Zhou, Z. *Cour. Forschungsinst. Senckenberg* **181**, 9–22 (1995).
8. Zhou, Z., Jin, F. & Zhang, J. *Chinese Sci. Bull.* **37**, 1365–1368 (1992).
9. Wellnhofer, P. *Archaeopteryx* **11**, 1–47 (1993).
10. Elzanowski, A. & Wellnhofer, P. *J. Vert. Paleontol.* **16**, 81–94 (1996).